MAGNITUDE MR IMAGE DENOISING VIA CURE-OPTIMIZED NON-LOCAL MEANS

Jung Ook Hong, Florian Luisier, and Patrick J. Wolfe

School of Engineering and Applied Sciences
Harvard University, Cambridge, MA 02138, USA

ABSTRACT

During their acquisition, magnetic resonance (MR) images are affected by random noise, causing the observed magnitude image samples to be Rician distributed. In order to reduce the noise level while preserving the relevant image features, we develop an optimized Non-Local Means (NLM) denoising algorithm. The most sensitive parameters of the proposed NLM estimator are optimized on the squared-magnitude image, which follows a non-central chi-square distribution on two degrees of freedom. This minimum MSE optimization is performed via the minimization of the so-called chi-square unbiased risk estimate (CURE). Taking advantage of some acceleration techniques involving convolutions and parallel computation, we show that the proposed CURE-optimized NLM outperforms some state-of-the-art NLM algorithms with no increase in computation time.

Index Terms— MR image denoising, Non-local means, Chi-square distribution, Rician distribution.

1 INTRODUCTION

Magnetic resonance (MR) imaging is a widely-used medical imaging technique that allows the visualization of the internal soft tissue of the body. The MR scanner provides a set of discrete Fourier samples, which are commonly assumed to be corrupted by complex additive white Gaussian noise (AWGN) [1]. After reconstruction (primarily through the inverse discrete Fourier transform), the magnitude MR image pixels are Rician distributed [2]. Contrary to the AWGN, the Rician "noise" has a signal-dependent mean and variance that makes its effective reduction more challenging. Note that the signal dependency of the bias disappears in the squared image, which follows a non-central chi-square distribution on two degrees of freedom, whose non-centrality parameter is proportional to the underlying noise-free squared magnitude.

Most successful AWGN denoising approaches (transform-based, image-domain filters,...) have been adapted to magnitude MR image denoising. Among these, the Non-Local Means (NLM) filter [3] has gained a lot of attention recently. NLM takes advantage of the redundancy between image patches. Each denoised pixel is obtained by a weighted average of pixels exhibiting similar (but not necessary local) neighborhoods (image patches).The weights are calculated from the photometric similarity between two patches centered around the current pixel and the reference one. The original NLM filter has then been refined by integrating a pre-selection feature which further decreases the contribution of unrelated pixels [4, 5]. The weights involved in the pre-selection are computed on a pre-estimated image (e.g., obtained by simple lowpass filtering).

The first adaptation of the NLM to magnitude MR data [6] consists of applying the original NLM, taking the square of the results, removing the constant bias, and finally getting back to the magnitude image domain. It has been later observed that better results can be obtained by weighting the squared-magnitude image, while still computing the weights in the magnitude domain [7, 8, 9].

In all the previous Rician adaptations of the NLM, the chi-square distribution of the squared data has only been exploited to correct for the bias. In this paper, we further exploit it by using the so-called "Chi-square Unbiased Risk Estimate" (CURE) recently introduced in [10]. CURE is a robust unbiased estimate of the expected mean-square error (MSE) between the (unknown) noise-free squared-magnitude image and a processed version of it. Since CURE only depends on the noisy squared-magnitude image, it can be computed in practice. It can then be used to optimize (in the minimum MSE sense) the parameters of a broad class of estimators of the noise-free image. Similar to [11] (AWGN) and [12] (Poisson noise), we propose to rely on CURE to optimize the most sensitive parameters of an adapted Rician NLM involving refined weights.

2 PRELIMINARIES

2.1 Noise in MR Images

Let $\Omega \subset \mathbb{Z}_+^2$ be the set of indices describing an $N_x \times N_y$ image domain. Let $\boldsymbol{\mu} = [\mu_{\boldsymbol{n}}]_{\boldsymbol{n}\in\Omega} \in \mathbb{C}^N$ contain the $N = N_x N_y$ samples of an $N_x \times N_y$ ideal (noise-free) MR image and $\boldsymbol{m} = [m_{\boldsymbol{n}}]_{\boldsymbol{n}\in\Omega} \in \mathbb{C}^N$ be its realistic (noisy) observation. In MR image acquisition, the statistical relationship between m_n and μ_n is given by

$$\begin{cases} \Re\{m_{\boldsymbol{n}}\} & \sim & \mathcal{N}(\Re\{\mu_{\boldsymbol{n}}\}, \sigma^2) \\ \Im\{m_{\boldsymbol{n}}\} & \sim & \mathcal{N}(\Im\{\mu_{\boldsymbol{n}}\}, \sigma^2) \end{cases} \tag{1}$$

where σ^2 is the variance of a (complex) additive white Gaussian noise.

We are interested in estimating the magnitude of $\mu_{\boldsymbol{n}}$; i.e., $|\mu_{\boldsymbol{n}}| = \sqrt{\Re\{\mu_{\boldsymbol{n}}\}^2 + \Im\{\mu_{\boldsymbol{n}}\}^2}$ from $|m_{\boldsymbol{n}}|$. Defining $\boldsymbol{x}$ and $\boldsymbol{y}$ as

$$\begin{cases} \boldsymbol{x} & = & \left[|\mu_{\boldsymbol{n}}|^2/\sigma^2\right]_{\boldsymbol{n}\in\Omega} \\ \boldsymbol{y} & = & \left[|m_{\boldsymbol{n}}|^2/\sigma^2\right]_{\boldsymbol{n}\in\Omega} \end{cases}, \tag{2}$$

our original estimation problem becomes that of finding a good (e.g. in the minimum MSE sense) estimator $\hat{\boldsymbol{x}} = \boldsymbol{f}(\boldsymbol{y})$ of $\boldsymbol{x}$ from $\boldsymbol{y}$. Contrary to $\boldsymbol{m}$, which is Rician distributed, $\boldsymbol{y}$ follows a non-central chi-square distribution with non-centrality parameter $\boldsymbol{x}$ and two degrees of freedom.

2.2 NLM for Magnitude MR Image Denoising

The first adaptation of the NLM to Rician noise was proposed by Manjón *et al.* [6]. It consists of applying the original NLM [3] to the magnitude MR image and then correcting for the bias in the squared-magnitude domain. The resulting estimator, called "Unbiased NLM" (UNLM) is given by $\hat{\boldsymbol{\mu}} = [\hat{\mu}_{\boldsymbol{n}}]_{\boldsymbol{n}\in\Omega}$, with

$$\hat{\mu}_{\boldsymbol{n}} = \sqrt{\max\left(\left(\frac{\sum_{\boldsymbol{k}\in\mathbb{Z}^2} w_{\boldsymbol{n},\boldsymbol{k}}|m_{\boldsymbol{n}+\boldsymbol{k}}|}{W_{\boldsymbol{n}}}\right)^2 - 2\sigma^2, 0\right)}, \tag{3}$$

where we have defined $W_{\boldsymbol{n}} = \sum_{\boldsymbol{k}\in\mathbb{Z}^2} w_{\boldsymbol{n},\boldsymbol{k}}$ as the normalization factor. The weights $w_{\boldsymbol{n},\boldsymbol{k}}$ penalize dissimilar image patches. The most

widely used measure of similarity is a weighted ℓ_2 distance; i.e.,

$$d_{\boldsymbol{n},\boldsymbol{k}} = \frac{1}{\sigma^2} \sum_{\boldsymbol{l}\in\mathbb{Z}^2} h(\boldsymbol{l}) \left(|m_{\boldsymbol{n}+\boldsymbol{k}+\boldsymbol{l}}| - |m_{\boldsymbol{k}+\boldsymbol{l}}|\right)^2, \tag{4}$$

where $h : \mathbb{Z}^2 \to \mathbb{R}$ is a kernel that satisfies $\sum_{\boldsymbol{l}\in\mathbb{Z}^2} h(\boldsymbol{l}) = 1$. The kernel h penalizes pixels that are geometrically far away from the center of the considered image patch. The weights are then given by

$$w_{\boldsymbol{n},\boldsymbol{k}} = I(\boldsymbol{k}) g_\lambda(d_{\boldsymbol{n},\boldsymbol{k}}), \tag{5}$$

where $I : \mathbb{Z}^2 \to \mathbb{R}$ is usually an indicator function that defines the search region; e.g., $I(\boldsymbol{k}) = \mathbf{1}_{[-S,\dots,S]^2}$ for a square-shaped search region with width $(2S+1)$, $S \in \mathbb{N}$. Some popular choices of weighting function $g : \mathbb{R}_+ \to [0,1]$ are

$$g_\lambda(x) = \exp(-x/\lambda) \quad \text{or} \quad g_\lambda(x) = \frac{\lambda^2}{\lambda^2 + x^2}, \tag{6}$$

where $\lambda > 0$ is a well-chosen smoothing parameter.

Another Rician-adapted NLM estimator has been considered in [7, 8, 9]. In these works, the weights are applied on the *squared* magnitude image. Using the notations introduced in (2) and defining

$$f_{\boldsymbol{n}}(\boldsymbol{y}) = \frac{\sum_{\boldsymbol{k}\in\mathbb{Z}^2} w_{\boldsymbol{n},\boldsymbol{k}} y_{\boldsymbol{n}+\boldsymbol{k}}}{W_n} - 2, \tag{7}$$

this so-called "Rician NLM" (RNLM) is expressed as

$$\hat{\mu}_{\boldsymbol{n}} = \sqrt{\sigma^2 \cdot \max\left(f_{\boldsymbol{n}}(\boldsymbol{y}), 0\right)}. \tag{8}$$

2.3 CURE: Chi-square Unbiased Risk Estimate

Most denoising algorithms involve several parameters, whose settings have a significant impact on the denoising quality. Ideally, these parameters should be set such as to minimize some cost function, the most popular being the (expected) MSE. The expected MSE for an estimator $\boldsymbol{f}(\boldsymbol{y})$ of $\boldsymbol{x}$ is defined as

$$\mathbb{E}\left\{\text{MSE}\right\} = \frac{1}{N} \sum_{\boldsymbol{n}\in\Omega} \left(\mathbb{E}\left\{f_{\boldsymbol{n}}(\boldsymbol{y})^2\right\} - \mathbb{E}\left\{2x_{\boldsymbol{n}} f_{\boldsymbol{n}}(\boldsymbol{y})\right\} + x_{\boldsymbol{n}}^2\right). \tag{9}$$

To be computed, it requires the knowledge of the true parameter $\boldsymbol{x}$, which is obviously not available in practice. Yet, similar to the additive white Gaussian (SURE) and Poisson (PURE) noise cases, it is also possible to derive a Stein-like unbiased estimate for non-central chi-square distributed data. Such an unbiased estimate of the expected MSE has been recently introduced in [10] and termed CURE. For any estimator $\boldsymbol{f}(\boldsymbol{y})$ satisfying some smoothness constraints, CURE is given by

$$\text{CURE} = \frac{1}{N} \sum_{\boldsymbol{n}\in\Omega} \Big[\left(f_{\boldsymbol{n}}(\boldsymbol{y}) - (y_{\boldsymbol{n}} - 2)\right)^2 - 4\left(y_{\boldsymbol{n}} - 1\right) + 8\left(\left(y_{\boldsymbol{n}} - 1\right)\partial f_{\boldsymbol{n}}(\boldsymbol{y}) - y_{\boldsymbol{n}} \partial^2 f_{\boldsymbol{n}}(\boldsymbol{y})\right) \Big] \tag{10}$$

where $\partial f_{\boldsymbol{n}}(\boldsymbol{y}) = \frac{\partial f_{\boldsymbol{n}}(\boldsymbol{y})}{\partial y_{\boldsymbol{n}}}$ and $\partial^2 f_{\boldsymbol{n}}(\boldsymbol{y}) = \frac{\partial^2 f_{\boldsymbol{n}}(\boldsymbol{y})}{\partial y_{\boldsymbol{n}}^2}$. Note that $\mathbb{E}\left\{\text{CURE}\right\} = \mathbb{E}\left\{\text{MSE}\right\}$.

As can be observed from (10), CURE can indeed be computed in practice as it only depends on the *observed* data $\boldsymbol{y}$. Note that its variance is inversely proportional to the number of measurements N, making CURE a robust unbiased estimate of the MSE in image processing applications.

3 RICIAN NON-LOCAL MEANS AND CURE

In this section, we derive the expression of CURE for the NLM estimator $\boldsymbol{f}(\boldsymbol{y})$ introduced in (7). Similar to [12], we consider a refined weighting function defined as

$$w_{\boldsymbol{n},\boldsymbol{k}} = \begin{cases} I(\boldsymbol{k}) g_{\lambda_1}(d_{\boldsymbol{n},\boldsymbol{k}}) g_{\lambda_2}(\tilde{d}_{\boldsymbol{n},\boldsymbol{k}}) & , \boldsymbol{k} \neq \boldsymbol{0} \\ w_{\boldsymbol{0}} & , \boldsymbol{k} = \boldsymbol{0} \end{cases}. \tag{11}$$

The similarity measure $d_{\boldsymbol{n},\boldsymbol{k}}$ introduced in (4) can be re-expressed in terms of the normalized squared magnitude data $\boldsymbol{y}$ as

$$d_{\boldsymbol{n},\boldsymbol{k}} = \sum_{\boldsymbol{l}\in\mathbb{Z}^2} h(\boldsymbol{l}) \left(y_{\boldsymbol{n}+\boldsymbol{k}+\boldsymbol{l}} + y_{\boldsymbol{n}+\boldsymbol{l}} - 2\sqrt{y_{\boldsymbol{n}+\boldsymbol{k}+\boldsymbol{l}} y_{\boldsymbol{n}+\boldsymbol{l}}}\right).$$

The similarity measure $\tilde{d}_{\boldsymbol{n},\boldsymbol{k}}$ is computed from pre-estimated data $\tilde{y}_{\boldsymbol{n}}$. These data are obtained by applying a smoothing kernel $\tilde{h}$ to the normalized magnitude data $\sqrt{y_{\boldsymbol{n}}}$; i.e.,

$$\tilde{y}_{\boldsymbol{n}} = \Big(\sum_{\boldsymbol{l}\in\mathbb{Z}^2} \tilde{h}(\boldsymbol{l}) \sqrt{y_{\boldsymbol{n}+\boldsymbol{l}}}\Big)^2,$$

leading to

$$\tilde{d}_{\boldsymbol{n},\boldsymbol{k}} = \tilde{y}_{\boldsymbol{n}+\boldsymbol{k}} + \tilde{y}_{\boldsymbol{n}} - 2\sqrt{\tilde{y}_{\boldsymbol{n}+\boldsymbol{k}} \tilde{y}_{\boldsymbol{n}}}.$$

The center weight $w_{\boldsymbol{0}} \in [0,1]$ is set to a constant value to avoid over-weighting effects [6]. We can then state the following two propositions.

Proposition 1. *The first-order partial derivatives of the NLM estimator* (7) *with respect to $y_{\boldsymbol{n}}$ are given by*

$$\partial f_{\boldsymbol{n}}(\boldsymbol{y}) = \frac{1}{W_n} \left(\sum_{\boldsymbol{k}\in\mathbb{Z}^2} (\partial w_{\boldsymbol{n},\boldsymbol{k}}) y_{\boldsymbol{n}+\boldsymbol{k}} - (f_{\boldsymbol{n}}(\boldsymbol{y}) + 2)\partial W_{\boldsymbol{n}} + w_{\boldsymbol{0}} \right). \tag{12}$$

Proposition 2. *The second-order partial derivatives of the NLM estimator* (7) *with respect to $y_{\boldsymbol{n}}$ are given by*

$$\partial^2 f_{\boldsymbol{n}}(\boldsymbol{y}) = \frac{1}{W_n} \Bigg(\sum_{\boldsymbol{k}\in\mathbb{Z}^2} (\partial^2 w_{\boldsymbol{n},\boldsymbol{k}}) y_{\boldsymbol{n}+\boldsymbol{k}} - 2\partial f_{\boldsymbol{n}}(\boldsymbol{y}) \partial W_{\boldsymbol{n}} - (f_{\boldsymbol{n}}(\boldsymbol{y}) + 2)\partial^2 W_{\boldsymbol{n}} \Bigg). \tag{13}$$

The expressions for the first- and second-order partial derivatives of the weights that appear in Proposition 1 and Proposition 2 can be found at `http://people.fas.harvard.edu/~johong/ISBI2012/Appendix.pdf`.

Proposition 1 and 2 allow us to compute the CURE (10) for the NLM estimator $\boldsymbol{f}(\boldsymbol{y})$ defined in (7) using the refined weights introduced in (11). When considering symmetric kernels h and $\tilde{h}$, the NLM can be efficiently implemented using convolutions as reported by Condat in [13]. This implementation reduces the computational complexity and enables the straightforward parallel computation of the weights and their partial derivatives. A sketch of the parallelized CURE-RNLM algorithm is shown in Algorithm 1.

Algorithm 1 CURE-RNLM

1. Initialization: $(W_{\boldsymbol{n}}, \partial W_{\boldsymbol{n}}, \partial^2 W_{\boldsymbol{n}}, f_{\boldsymbol{n}}, \partial f_{\boldsymbol{n}}, \partial^2 f_{\boldsymbol{n}}) \leftarrow 0$.
2. **parallel for** $\boldsymbol{k} \in ([-S,\dots,S] \times [-S,\dots,S]) \backslash [0,0]$,
   for $\boldsymbol{n} \in \Omega$,
   $W_{\boldsymbol{n}} \leftarrow W_{\boldsymbol{n}} + w_{\boldsymbol{n},\boldsymbol{k}}$; $f_{\boldsymbol{n}} \leftarrow f_{\boldsymbol{n}} + w_{\boldsymbol{n},\boldsymbol{k}} y_{\boldsymbol{n}+\boldsymbol{k}}$
   $\partial W_{\boldsymbol{n}} \leftarrow \partial W_{\boldsymbol{n}} + \partial w_{\boldsymbol{n},\boldsymbol{k}}$; $\partial f_{\boldsymbol{n}} \leftarrow \partial f_{\boldsymbol{n}} + \partial w_{\boldsymbol{n},\boldsymbol{k}} y_{\boldsymbol{n}+\boldsymbol{k}}$
   $\partial^2 W_{\boldsymbol{n}} \leftarrow \partial W_{\boldsymbol{n}}^2 + \partial^2 w_{\boldsymbol{n},\boldsymbol{k}}$; $\partial^2 f_{\boldsymbol{n}} \leftarrow \partial^2 f_{\boldsymbol{n}} + \partial^2 w_{\boldsymbol{n},\boldsymbol{k}} y_{\boldsymbol{n}+\boldsymbol{k}}$
   end
   end
3. **for** $\boldsymbol{n} \in \Omega$,
   a. $W_{\boldsymbol{n}} \leftarrow W_{\boldsymbol{n}} + w_{\boldsymbol{0}}$; $f_{\boldsymbol{n}} \leftarrow f_{\boldsymbol{n}} + w_{\boldsymbol{0}} y_{\boldsymbol{n}}$
   b. Normalize $f_{\boldsymbol{n}}$ as in (7).
   c. Calculate $\partial f_{\boldsymbol{n}}$ and $\partial^2 f_{\boldsymbol{n}}$ via (12) and (13).
   d. Obtain $\hat{\mu}_{\boldsymbol{n}}$ via (8).
   end
4. Compute CURE via (10).

4 CURE-OPTIMIZED RNLM ALGORITHM

The NLM involves numerous parameters: the size of the search region S, shape of the kernels h and $\tilde{h}$, smoothing parameters λ_1 and λ_2, value of the center weight $w_{\mathbf{0}}$, shape of the weight functions $g_{\lambda_1}(\cdot)$ and $g_{\lambda_2}(\cdot)$. These various parameters could be jointly optimized by minimizing CURE. Here, we restrict ourselves to the joint optimization of the smoothing parameters, as these usually have the greatest impact on the denoising performances [3, 11, 12].

In Fig. 1(A), we show a plot of CURE as a function of λ_1 and λ_2. As observed (and verified in further experiments), the minimum of CURE always occurs in a rather flat region. This suggests that several couples (λ_1, λ_2) can achieve similar performances. Consequently, we propose to fix $\lambda_2 = \alpha\lambda_1$ and only optimize λ_1. In practice, we found that the choice $\alpha = 3\sum_{\boldsymbol{l}\in\mathbb{Z}^2} \tilde{h}(\boldsymbol{l})^2$ matches the results obtained by the joint optimization of λ_1 and λ_2.

In Fig. 1(B), we display the MSE and CURE curves as a function of the smoothing parameter λ_1. As observed, CURE can indeed be considered as a robust estimator of the MSE and subsequently minimized to obtain the MMSE value of the smoothing parameters.

(A) **(B)**

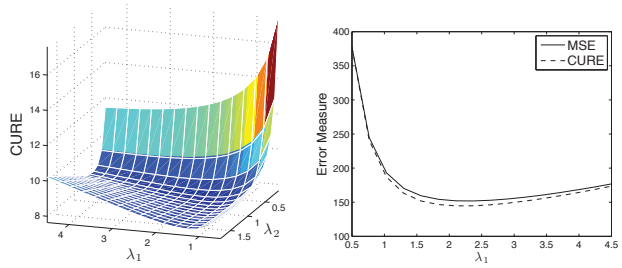


Fig. 1: **(A)** CURE as a function of λ_1 and λ_2 ($\sigma = 20$). **(B)** CURE vs. MSE as a function of λ_1 ($\sigma = 20$).

To efficiently optimize the nonlinear parameter λ_1, we could consider Newton's method as in [12]. Yet, this would require the computation of the first- and second-order derivatives of CURE with respect to λ_1. To avoid this additional computational burden, we perform a golden section search, which only requires the evaluation of CURE for a few values of λ_1. In practice, the optimal value is usually reached after 10 iterations, each iteration involving two computations of CURE.

5 EXPERIMENTS

5.1 Simulated data

In this section, we evaluate the performance of the proposed CURE-optimized RNLM. As benchmarks, we report the results obtained by the UNLM (3) described in [6] (MATLAB code downloadable at `http://personales.upv.es/jmanjon/denoising/nlm2d.htm`, Version 1.0) and by an instance of RNLM (7) implemented by Manjón *et al.* (MATLAB code downloadable at the same url, Version 2.0). The parameters of these two algorithms are reported in Table 1. We have implemented two variants of our algorithm, denoted CURE-RNLM$_1$ and CURE-RNLM$_2$. In the first, we use the same set of parameters as the RNLM implemented by Manjón, except for the weight function $g_{\lambda_2}(\cdot)$, which is chosen to be continuously differentiable. In the second variant, we opt for a different set of parameters. In both variants, the smoothing parameter λ_1 is optimized with CURE and $\lambda_2 = \alpha\lambda_1$.

The synthetic magnitude MR images used in the experiments are the median sagittal, coronal, and transverse section of a brain obtained from BrainWeb [14]. To evaluate the denoising performance of the various algorithms, each image is corrupted with various levels σ of

Params	UNLM [6]	RNLM	CURE-RNLM$_1$	CURE-RNLM$_2$
S	5	5	5	7
h	pyramidal 5×5	pyramidal 5×5	pyramidal 5×5	Gaussian $\sigma_h = 3$
$\tilde{h}$	N/A	uniform 3×3	uniform 3×3	Gaussian $\sigma_{\tilde{h}} = 1$
λ_1	1.2^2	1.4^2	CURE-optimized	CURE-optimized
λ_2	N/A	1	$\alpha\lambda_1$	$\alpha\lambda_1$
$w_{\mathbf{0}}$	max	0.5	0.5	0.25
$g_{\lambda_1}(x)$	e^{-x/λ_1}	$\frac{\lambda_1^2}{\lambda_1^2+x^2}$	$\frac{\lambda_1^2}{\lambda_1^2+x^2}$	$\frac{\lambda_1^2}{\lambda_1^2+x^2}$
$g_{\lambda_2}(x)$	1	$\begin{cases} 1, & x < \lambda_2 \\ 0, & \text{otherwise} \end{cases}$	$\frac{\lambda_2^2}{\lambda_2^2+x^2}$	$\frac{\lambda_2^2}{\lambda_2^2+x^2}$

Table 1: Parameters used in the various NLM algorithms.

Rician noise, which are assumed to be known. The denoising quality is quantified in terms of the peak signal-to-noise ratio (PSNR), defined as

$$\text{PSNR} = 10\log_{10}\frac{N\|\boldsymbol{\mu}\|_\infty^2}{\|\hat{\boldsymbol{\mu}} - \boldsymbol{\mu}\|^2}.$$

The results obtained by the various algorithms are displayed in Table 2. As observed, our CURE-optimized RNLMs consistently outperform the hand-optimized UNLM and RNLM. The average gain is around $+0.2$ dB for our CURE-RNLM$_1$ and about $+0.6$ dB for our CURE-RNLM$_2$. The gains are more significant at low input PSNR, where the Rician characteristic of the noise is more pronounced. The second variant of our CURE-RNLM usually achieves the highest PSNRs. This suggests that further gains could be obtained through a joint CURE optimization of all the parameters involved in the NLM and reported in the first column of Table 1.

We have also reported in Table 2 the oracle performances achieved by our RNLM estimators (PSNRs shown in parentheses). These are obtained by selecting the smoothing parameter λ_1 to minimize the image-domain MSE. As observed, these optimal results are within 0.07 dB from those obtained by the CURE optimization. This means that the nonlinear mapping (8) required to get the final magnitude-image estimate $\hat{\boldsymbol{\mu}}$ mostly preserves the MSE optimality of the squared-image estimate $\hat{\boldsymbol{x}}$.

	σ	Input PSNR	UNLM [6]	RNLM	CURE-RNLM$_1$	CURE-RNLM$_2$
Sagittal	5	33.49	38.82	39.36	**39.53** (*39.54*)	39.51 (*39.52*)
	10	27.46	34.84	35.30	35.35 (*35.38*)	**35.63** (*35.64*)
	20	21.47	29.37	30.38	30.55 (*30.58*)	**31.14** (*31.15*)
	30	18.00	25.89	27.41	27.63 (*27.64*)	**28.19** (*28.19*)
	50	13.53	21.11	23.76	23.98 (*24.01*)	**24.23** (*24.27*)
Coronal	5	33.56	38.35	39.02	**39.22** (*39.22*)	39.19 (*39.19*)
	10	27.52	34.60	34.94	35.02 (*35.04*)	**35.30** (*35.30*)
	20	21.50	29.39	30.08	30.25 (*30.29*)	**30.86** (*30.87*)
	30	18.00	26.10	27.06	27.29 (*27.33*)	**27.89** (*27.93*)
	50	13.58	21.69	23.36	23.63 (*23.66*)	**23.96** (*23.99*)
Transverse	5	33.12	38.43	39.13	**39.45** (*39.46*)	39.44 (*39.44*)
	10	27.09	35.05	35.04	35.12 (*35.14*)	**35.45** (*35.45*)
	20	21.06	29.86	30.21	30.30 (*30.34*)	**31.01** (*31.01*)
	30	17.54	26.62	27.11	27.29 (*27.33*)	**28.09** (*28.10*)
	50	13.10	22.31	23.19	23.38 (*23.45*)	**24.01** (*24.07*)

Table 2: PSNR of the various algorithms, averaged over 10 noise realizations. Best results are shown in boldface and oracle results in italic.

5.2 Real data

We have applied the proposed CURE-RNLMs to real magnitude MR images of an adult knee and of an infant brain. The knee image, shown in Fig. 2(A), consists of a 512×512 16-bit image acquired on a Siemens 1.5T Magnetom, following a T2-weighted protocol. The newborn brain image displayed in Fig. 2(B) is a 256×176 16-bit slice extracted from a $256 \times 144 \times 176$ 3D volume acquired on a Siemens 3T Magnetom, following a T1-weighted protocol. In these real images, the noise level σ is estimated from the background $\mathcal{B}$ as $\hat{\sigma} = \sqrt{\frac{1}{2} \sum_{\boldsymbol{n} \in \mathcal{B}} |m_{\boldsymbol{n}}|^2}$.

As observed in Fig. 2(C) and 2(D), the proposed CURE-RNLM considerably reduces the noise level, without oversmoothing nor introducing unpleasant denoising artifacts. Fine relevant features are thus still preserved.

5.3 Computation times

All algorithms are fully implemented in MATLAB R2010b without the use of pre-compiled 'mex' files. On an Intel CPU with quad cores (2.33 GHz), the computation time for UNLM and RNLM is 273 s and 121 s, respectively, for a 512×512 image with the set of parameters provided in Table 1. In contrast, the first variant of our proposed method, CURE-RNLM$_1$, takes about 3.5 s for one evaluation of CURE, due to the parallelization mentioned in Algorithm 1. CURE-RNLM$_2$, which uses larger kernel and search region sizes, takes about 124 s in total (6.2 s per CURE evaluation). This is comparable to the un-optimized RNLM of Manjón, which considers a 11×11 search region only.

6 CONCLUSION

We have proposed an optimized Rician Non-Local Means estimator for the adaptive denoising of magnitude MR images. We have considered refined weights involving two smoothing parameters. Their values have been set such as to minimize CURE, which is a reliable estimate of the squared image-domain MSE. Indeed, the PSNR results obtained by the proposed CURE-RNLM match the oracle performances achievable by an MMSE selection of the smoothing parameters. Consequently, the proposed optimized RNLMs favorably compare with other Rician adaptations of the original NLM filter. Promising results on real magnitude MR data have been obtained. We are currently working on the 3D extension of the proposed approach, as well as on its more efficient parallel implementation.

7 ACKNOWLEDGEMENTS

This work was supported by the Swiss National Science Foundation Fellowship PBELP2-133245.

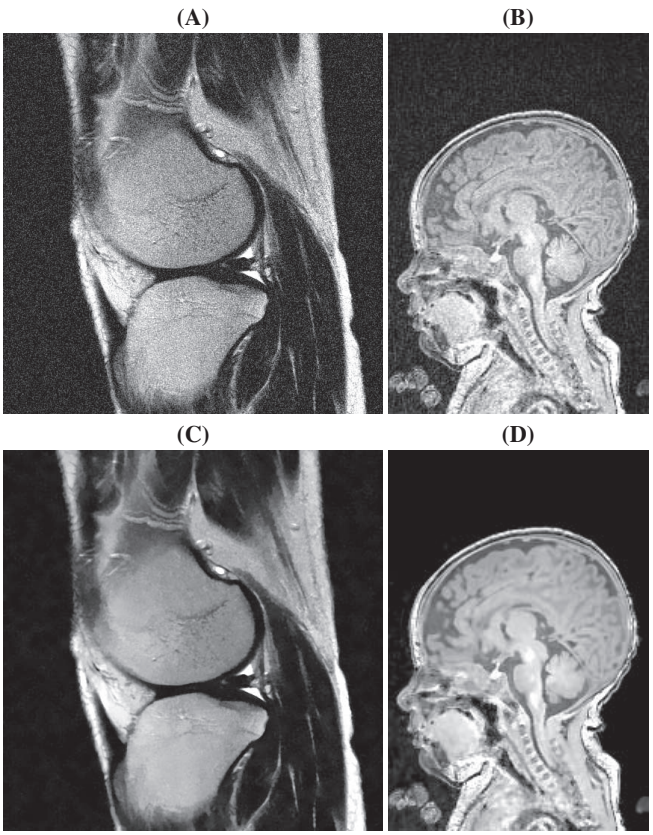


Fig. 2: **(A)** Real knee image, $\hat{\sigma} = 39.3$, courtesy of Dr. Laura Gui, University of Geneva. **(B)** Real infant brain image, $\hat{\sigma} = 18.5$, courtesy of Prof. Wen-Yih Isaac Tseng, NTUH. **(C)–(D)** Denoised with the proposed CURE-RNLM$_2$.

8 REFERENCES

[1] R. M. Henkelman, "Measurement of signal intensities in the presence of noise in MR images," *Med. Phys.*, vol. 12, no. 2, pp. 232–233, 1985.

[2] H. Gudbjartsson and S. Patz, "The Rician distribution of noisy MRI data," *Magn. Reson. Med.*, vol. 34, pp. 910–914, 1995.

[3] A. Buades, B. Coll, and J.-M. Morel, "A non-local algorithm for image denoising," *Proc. IEEE Comput. Soc Conf. Comput. Vis. Pattern Recognit.*, vol. 2, pp. 60–65, 2005.

[4] M. Mahmoudi and G. Sapiro, "Fast image and video denoising via non-local means of similar neighborhoods," *IEEE Signal Process. Lett.*, vol. 12, pp. 839–842, 2005.

[5] C. Kervrann and J. Boulanger, "Optimal spatial adaptation for patch-based image denoising," *Image Processing, IEEE Transactions on*, vol. 15, no. 10, pp. 2866–2878, Oct. 2006.

[6] J. Manjón, J. Carbonell-Caballero, J. Lull, G. García-Martí, L. Martí-Bonmatí, and M. Robles, "MRI denoising using non-local means," *Med. Image Anal.*, vol. 12, pp. 514–523, 2008.

[7] N. Wiest-Daesslé, S. Prima, P. Coupé, S. Morrissey, and C. Barillot, "Rician noise removal by non-local means filtering for low signal-to-noise ratio MRI: Applications to DT-MRI," *Proc. Med. Image Comput. Comput. Assist. Interv.*, pp. 171–179, 2008.

[8] J. Manjón, P. Coupé, L. Martí-Bonmatí, D. Collins, and M. Robles, "Adaptive non-local means denoising of MR images with spatially varying noise levels," *J. Magn. Reson. Imaging*, vol. 31, pp. 192–203, 2010.

[9] H. Liu, C. Yang, N. Pan, E. Song, and R. Green, "Denoising 3D MR images by the enhanced non-local means filter for Rician noise," *Magn. Reson. Imaging*, vol. 28, pp. 1485–1496, 2010.

[10] F. Luisier and P. Wolfe, "Chi-square unbiased risk estimate for denoising magnitude MR images," *Proc. IEEE Int. Conf. Image Proc.*, pp. 1593–1596, 2011.

[11] D. Van De Ville and M. Kocher, "SURE-Based Non-Local Means," *IEEE Signal Process. Lett.*, vol. 16, pp. 973–976, 2009.

[12] C.-A. Deledalle, F. Tupin, and L. Denis, "Poisson NL means: Unsupervised non-local means for Poisson noise," *Proc. Int. Conf. Image Proc.*, pp. 801–804, 2010.

[13] L. Condat, "A simple trick to speed up and improve the non-local means," Tech. Rep. hal-00512801, 2010.

[14] C. Cocosco, V. Kollokian, K. Remi, G. Pike, and A. Evans, "Brainweb: Online interface to a 3D MRI simulated brain database," *Neuroimage*, 1997.